Available online at www.sciencedirect.com
ScienceDirect
Journal of Nuclear Materials 366 (2007) 216–222
journal of nuclear materials
www.elsevier.com/locate/jnucmat

Effect of oxygen on fouling behavior in lead–bismuth coolant systems

Fenglei Niu [a,*], Robert Candalino [b], Ning Li [a]

[a] The Condensed Matter and Thermal Physics Group, Los Alamos National Laboratory, Los Alamos, NM 87545, USA
[b] Department of Nuclear Engineering, Texas A&M University, College Station, TX 77843-3133, USA

Received 27 July 2006; accepted 16 January 2007

Abstract

This experimental research investigates the effects of the oxygen in lead–bismuth eutectic on fouling. The analysis was carried out by performing three tests with different oxygen concentration on the recuperator where the heat transfer rate is susceptible to fouling, and introducing a correlation for the fouling factor. The comparison of fouling factors obtained with each oxygen level is presented, the relationship between fouling factors and oxygen concentrations is correlated, and the effects of oxidation on heat transfer are demonstrated qualitatively by wetting conditions of the samples.

1. Introduction

Liquid lead and lead–bismuth eutectic (LBE) are being considered as candidates for Gen IV reactor coolant and spallation neutron targets in accelerator-driven transmutation systems for their favorable thermal–physical and chemical properties. These properties include high boiling temperature, low melting point, high thermal conductivity, low viscosity, low neutron capture and moderation, and high spallation neutron yield. One of the main problems in using LBE is its adverse effect on structural materials. This liquid–metal dissolves many stainless steel alloying components that can lead to severe corrosion. A method to prevent corrosion in LBE systems is to create and maintain a protective oxide film on the surface of the stainless steel. Formation and longevity of this protective film depends on the oxygen concentration in the liquid–metal [1]. However, during high-oxygen concentration operation or even normal operation, the inner surfaces are often subject to fouling by fluid impurities, oxide formation, or other reactions between the fluid and the wall material. The subsequent deposition of a film or scale on the surface can greatly increase the resistance to heat transfer between the fluid and the wall. This effect can be treated by introducing an additional thermal resistance termed the *fouling factor*. Its value depends on many factors, such as operating temperature, oxygen concentration, and fluid velocity.

The fouling behavior has received considerable attention since it is a major and still unresolved problem in heat exchanger operation. Many widely

* Corresponding author. Tel.: +1 505 606 1440; fax: +1 505 667 7443.
E-mail address: fniu@lanl.gov (F. Niu).

0022-3115/$ - see front matter © 2007 Elsevier B.V. All rights reserved.
doi:10.1016/j.jnucmat.2007.01.223

Nomenclature

A	area (m^2)
C	concentration (wt%)
c_p	specific heat (J/kg K)
D	diameter (m)
h	convection heat transfer coefficient (W/m^2 K)
k	thermal conductivity (W/mK)
L	length of tubes (m)
$\dot{m}$	mass flow rate (kg/s)
n	number of tubes
Nu	Nusselt number
P	pitch (m)
Pe	Peclet number ($RePr$)
q	heat transfer rate (W)
R''_f	fouling factor (m^2 K/W)
T	fluid temperature (K)
ΔT_{LMTD}	logarithmic mean temperature difference (K)
U	overall heat transfer coefficient (W/m^2 K)

Subscripts

c	cold fluid
h	hot fluid
i	inlet or inside
m	mean value
n	nominal
o	outlet or outside
O	oxygen
s	shell
t	tube

accepted fouling models are based on the mass balance equation first proposed by Kern and Seaton [2]. In this equation the rate of fouling deposition depends on the type of fouling mechanism such as sedimentation, and crystallization while the rate of fouling removal depends on both the adhesive strength of the deposit and the shear stress, as well as the system configuration. In the oil industry, Ebert and Panchal [3] gave an equation to evaluate the growth of fouling for crude oil streams. In this equation, the fouling depends on the effects of velocity, film temperature, and the shear stress. In the nuclear industry, major researches about the fouling were performed in studying its effect on thermal-hydraulic characteristics of heat exchangers and steam generators. Schwarz [4] studied the heat transfer of Siemens PWR steam generators over long-term operation and suggested to correlate fouling factor to the amount of iron ingress which accumulated and adhered to the tube surface. Somerscales et al. [5] developed a novel technique to measure the thermal resistance of aqueous corrosion products formed on heated metal surfaces. Based on their experimental evidence, they found that in situations where damage to metal is not important the corrosion products could introduce a significant resistance to the heat transfer between flowing water and the metal surface. An extensive review, which includes the equipment and methods used in fouling studies, was given by Melo and Pinheiro [6]. To date, the basic phenomena of fouling are still under investigation and the use of mathematical models for prediction requires significant contributions from experiments and analyses. If we knew both the thickness and the thermal conductivity of the fouling, we could treat the heat transfer problem simply as another conduction resistance in series with the wall. In general, we know neither of these quantities and the only possible technique is to introduce the additional resistance as fouling factors in computing the overall heat transfer coefficient. This paper is concerned with a type of fouling that has received little attention in the past in spite of its importance to liquid–metal heat transfer equipment. This fouling is due to oxidation products that form on heat transfer surfaces exposed to liquid–metal. The objective is to obtain qualitative and quantitative information on the oxidation effects on fouling, which occurs in LBE systems using oxygen as a means of corrosion mitigation.

The experiments were performed in the DELTA (Development of Lead-Alloy Technology & Applications) Loop at the Los Alamos National Laboratory, as shown in Fig. 1. This loop was designed to study the long-term corrosive effects of LBE on structural materials at temperatures up to 550 °C, as well as the thermal and hydraulic properties of LBE. Prior to operation, LBE is heated to 300 °C in the melt tank and then transferred by helium pressure into the sump tank. A centrifugal pump submerged in the liquid–metal in the sump tank circulates the fluid through the loop. Detailed

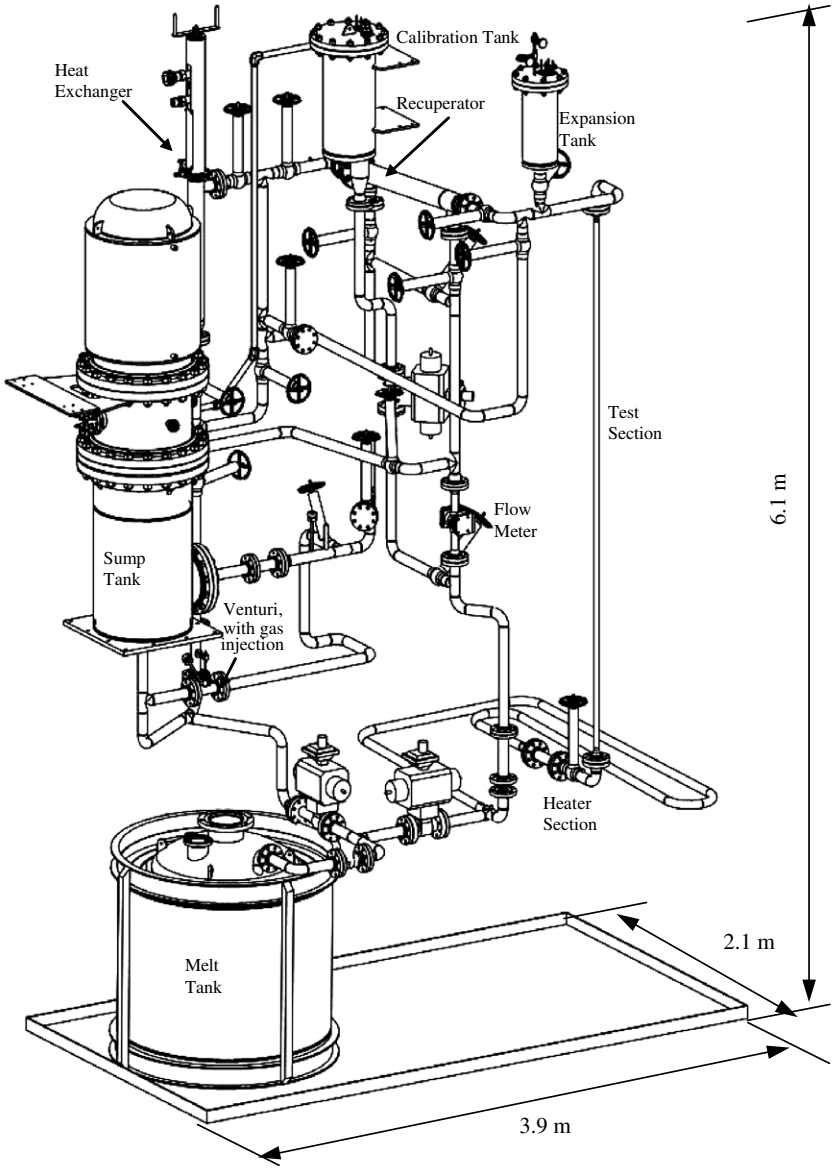

Fig. 1. Illustration of the DELTA Loop.

information about the DELTA Loop and its operations is provided in Ref. [7].

The test focuses on the heat transfer performance in a recuperator, which is installed in the DELTA loop. This is a shell-and-tube recuperator that is used to transfer heat between two counter-flowing LBE streams. Heat is transferred from the hot-side LBE prior to entering the heat exchanger, which reduces the heat removal load on the heat exchanger. It is then transferred to the cold-side LBE prior to entering the heat input section, which reduces the load required in the heat input section.

The shell is made of 4 in. schedule 80 pipes (10.2 cm I.D.). There are 19 tubes (1.43 cm O.D., 0.09 cm wall thickness) within the shell. The recuperator is configured in a counter-flow arrangement as shown in Fig. 2. The cold LBE flows on the shell side and the hot LBE flows on the tube side [8].

2. Analysis

Assuming negligible heat loss from the recuperator to its surroundings, the heat transfer rate can be expressed as:

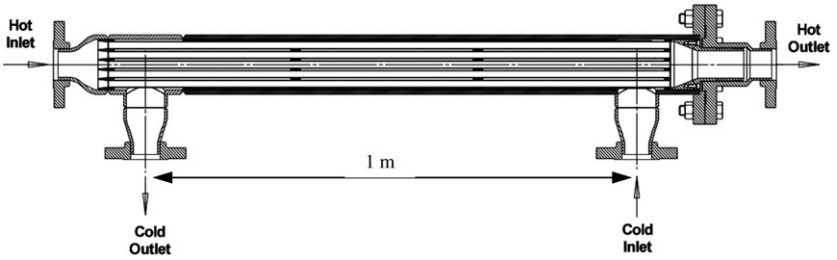

Fig. 2. Sectional view of recuperator.

$$q = \dot{m}_h c_{p,h}(T_{h,i} - T_{h,o}) = \dot{m}_c c_{p,c}(T_{c,o} - T_{c,i}), \quad (1)$$

where $\dot{m}$ is the mass flow rate, c_p is the specific heat, and T is the fluid temperature. Since this is a long, thin heat exchanger (the distance between the cold inlet and outlet is about 20 times of the inlet/outlet diameter), the cross flow near the inlet and outlet can be neglected and the heat exchanger basically operates in a counter-current configuration. Then the heat transfer rate can be calculated with

$$q = UA\Delta T_{LMTD}, \quad (2)$$

where U is the overall heat transfer coefficient, A is the heat transfer area, and ΔT_{LMTD} is the logarithmic mean temperature difference. The overall heat transfer coefficient can be expressed as [9]:

$$\frac{1}{UA} = \frac{1}{h_h A_h} + \frac{R''_{f,h}}{A_h} + \frac{\ln(D_{t,o}/D_{t,i})}{2\pi kL \cdot n} + \frac{R''_{f,c}}{A_c} + \frac{1}{h_c A_c}, \quad (3)$$

where R''_f is the fouling factor, L is the length of tubes, n is the number of tubes, and $D_{t,i}$ and $D_{t,o}$ are I.D. and O.D. of the tubes, respectively.

Since both sides of the tubes are contacting the same liquid–metal, we can define the fouling factor on two area bases as:

$$\frac{1}{UA} = \frac{1}{h_h A_h} + \frac{\ln(D_{t,o}/D_{t,i})}{2\pi kL \cdot n} + \frac{1}{h_c A_c} + \frac{R''_f}{A_n}, \quad (4)$$

where the nominal area A_n is given by:

$$A_n = \frac{A_h A_c}{A_h + A_c}. \quad (5)$$

Based on the design flow rate of the DELTA Loop, the assumption of fully developed turbulent flow can be properly made in both the tube side and shell side of the recuperator.

For the hot tube side of the recuperator, the heat transfer coefficient can be calculated by Seban–Shimazaki formula [10]:

$$Nu_h = 5.0 + 0.025 Pe_m^{0.8}, \quad (6)$$

where $Pe_m = Re_m Pr_m$ and the subscript m indicates that the fluid properties are evaluated at the mean bulk temperature $T_m = (T_{in} + T_{out})/2$. Eq. (6) is valid for $Pe_m > 100$ and $L/D_h > 60$. Although it was derived for a constant wall temperature, it has been recommended for a constant heat flux in systems free from oxide impurity and gas entrainment. Further discussion can be found in Reed's extensive review [11]. For the DELTA recuperator, $Pe_m > 500$ and $L/D_h = 93$, so Eq. (6) can be ideally used to calculate h_h in Eq. (4) which represents the heat transfer coefficient for a clean, unfinned surface.

For the cold side, the flow area is in between the inside surface of the shell and the outside surface of 19 tubes, as shown in Fig. 2. The hydraulic diameter can be obtained by:

$$D_{hydraulic} = \frac{D_{s,i}^2 - nD_{t,o}^2}{D_{s,i} + nD_{t,o}}, \quad (7)$$

where $D_{s,i}$ is the I.D. of the shell. For the fully developed turbulent flow, the heat transfer for the liquid–metal flowing through tube bundles can be evaluated by this empirical equation [12]:

$$Nu_c = 6.66 + 3.126\left(\frac{P}{D_{t,o}}\right) + 1.184\left(\frac{P}{D_{t,o}}\right)^2 + 0.0155(\Psi Pe)^{0.86}, \quad (8)$$

where P is the pitch between two centers of the tubes and Ψ is the ratio between eddy diffusivities of heat and momentum. Based on the comparison of analytical predictions with experimental results carried out by Dwyer [12], one can take $\Psi = 1$ in the range $Pe > 500$.

From Eqs. (1), (2), and (4), we can get explicitly the correlation for the fouling factor:

$$R''_f = \left(\frac{\Delta T_{LMTD}}{\dot{m}_h c_{p,h}(T_{h,i} - T_{h,o})} - \frac{1}{h_h A_h} - \frac{\ln(D_{t,o}/D_{t,i})}{2\pi kL \cdot n} - \frac{1}{h_c A_c}\right) \times \frac{A_h A_c}{A_h + A_c}. \quad (9)$$

Entering the experimental data and design parameters into the above equations, we calculated the fouling factors for each test. Eq. (9) enables us to investigate the effects of thermal and chemical factors such as temperature, flow rate, and oxygen concentration on the fouling factor and therefore the heat transfer between liquid–metal and pipes.

3. Experimental results

The oxygen control system consists of oxygen sensors, gas injection devices, and filters. There are three locations for gas injection in the loop: the sump volume, the expansion tank at the highest point, and in a bypass loop where a venturi section has inlet holes for the addition of gases. Introducing an oxygen–helium mixture (He–6 wt% O_2) into LBE will increase dissolved oxygen, while adding a hydrogen–helium mixture (He–4 wt% H_2) tends to remove dissolved oxygen from the liquid–metal in the form of water vapor. We have designed and built sensors that measure oxygen content by measuring the voltage developed across certain ceramics when a difference in oxygen concentration also exists across it [13]. The measured voltage depends on the ratio of the oxygen concentration in LBE to that at the reference electrode. Relationship between voltage and oxygen concentration is derived from formulas [1] and oxygen sensors are calibrated ahead of use in separate experiments. Data was collected and examined from three runs. For the first run, only hydrogen–helium mixture was injected in order to get the lowest oxygen concentration. For the next two runs, an oxygen–helium mixture was introduced in an attempt to have the system operate at higher oxygen levels. Table 1 gives the average temperatures and flow rates in the recuperator for the three runs.

The three runs operated with an average oxygen concentration of 4.64×10^{-7} wt%, 1.63×10^{-5} wt%, and 5.84×10^{-5} wt%, typically representing the low, medium, and high oxygen content in LBE within the temperature range 395–520 °C. The fouling factor increases significantly with the oxygen concentration in the range of 1.0×10^{-5} wt% because in this range the oxide layers begin to form. The experimental data can be well correlated by:

$$R''_{\mathrm{f}} = 2\times10^{-4}C_{\mathrm{O}}^{0.1514}, \tag{10}$$

where C_{O} is the oxygen concentration in wt%. Fig. 3 gives the experimental data with their correlation.

The oxygen dissolved in LBE can form oxide layers on the pipe wall, which not only increases the thermal resistance for conduction, but also makes it more difficult for the coolant to wet pipe surfaces, both of which contribute to the fouling. Following an extensive amount of experimental investigation on the effects of wetting on liquid–metal heat transfer, the wetting or lack of wetting does not significantly affect liquid–metal heat transfer. However, non-wetting combinations of liquid–metals and solid surfaces can suffer more readily from gas-entrainment problems at the solid–liquid interface; impurities and particles can more easily become trapped at a non-wetting solid–liquid interface, thus greatly reducing heat transfer [11]. The oxide-layer structure of steel in a liquid-lead alloy with oxygen control principally depends on steel composition, temperature, and hydraulic factors. For temperatures below 550 °C, a 10–20 μm external magnetite (Fe_3O_4) layer and a compact internal spinel ($(Fe,Cr)_xO_4$) layer of roughly equal thickness are generated on the pipe surface [14]. This duplex-layer can protect steels from corrosion.

Since the DELTA Loop had been in operations for over several thousands of hours, the growth of the oxide layers on the pipe walls should have become very small. For the durations and temperatures of the tests, it is reasonable to assume that the oxides do not change, and the approximate total thickness is about 20 μm.

The thermal conductivity of magnetite at temperatures within the range 340–657 K is given by this equation [15]:

$$k_{\mathrm{magnetite}} = 4.23 - 1.37\times10^{-3}T\ (\mathrm{W/m\ K}), \tag{11}$$

where T is in unit K. For the spinel at temperatures from 100 to 1325 °C, Headrick et al. [16] measured the thermal conductivity by the laser flash method. The experimental data can be correlated by:

Table 1
Temperatures and flow rates for the three runs

Run	$T_{\mathrm{c,i}}$ (°C)	$T_{\mathrm{c,o}}$ (°C)	$T_{\mathrm{h,i}}$ (°C)	$T_{\mathrm{h,o}}$ (°C)	$\dot{V}$ (m^3/h)	t (h)
1	436.9	495.8	519.8	461.1	4.38	18.2
2	395.1	430.0	446.3	410.5	3.87	39.3
3	403.9	417.7	426.4	412.6	4.79	24.0

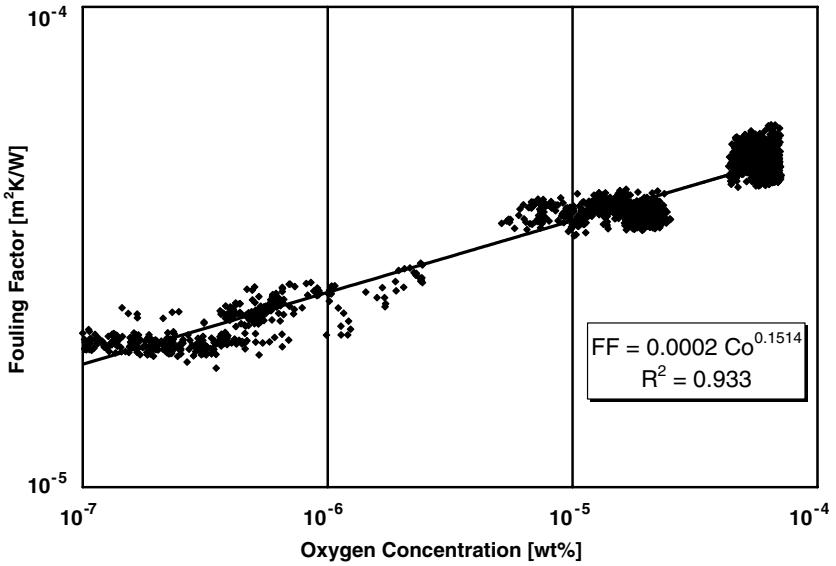

Fig. 3. Fouling factor vs. oxygen concentration.

$$k_{\text{spinel}} = 50.78T^{-0.36}\ (\text{W/m K}), \tag{12}$$

where T is in °C. The comparison of thermal resistances for conduction, convection, and fouling, which were calculated from the experimental data and empirical equations, is shown in Table 2.

Observations of the inside surface of the test section pipes confirm that the wetting condition is worsened by the dissolved oxygen. Fig. 4(a) shows the interior of the pipe following the first run in which the oxygen concentration is very low. The traces of the frozen LBE indicate the pipe has once experienced good wetting under the low oxygen level. However, the extent of adherence, as shown in Figs. 4(b) and 4(c) after Runs 2 and 3, respectively, decreases significantly with higher oxygen concentrations. So the introduction of oxygen does reduce wetting in the pipe over time.

If the oxide thickness is 80 μm, a hypothetical value reached in long-term operations. The thermal resistance due to oxide film can make up about 12.3% of total thermal resistance for a 1 mm thick fuel cladding. However, if the oxygen concentration is saturated at 550 °C, $C_O = 1.17 \times 10^{-3}$ wt%. Based on Eq. (10), $R''_f = 7.20 \times 10^{-5}$ m² K/W. Then from Eq. (4) the thermal resistance from the fouling is 1.56×10^{-4} K/W, making up 40.8% of total thermal resistance. This case will happen when the liquid–metal is exposed to air for a long time or there is considerable absorption of oxygen from oxides on piping. The fouling can contribute much more to the total thermal resistance and will reach its

Table 2
Comparison of the thermal resistances of the conduction, convection, and fouling based on the results of three tests at different oxygen concentrations

		Test 1 $C_O = 4.64 \times 10^{-7}$ (wt%) 437–520 °C		Test 2 $C_O = 1.63 \times 10^{-5}$ (wt%) 395–446 °C		Test 3 $C_O = 5.84 \times 10^{-5}$ (wt%) 404–526 °C	
		Thermal resistance (K/W)	Percent of total	Thermal resistance (K/W)	Percent of total	Thermal resistance (K/W)	Percent of total
Conduction		4.83×10^{-5}	17.1	4.83×10^{-5}	15.0	4.83×10^{-5}	14.5
Convection (cold)		7.91×10^{-5}	27.8	7.98×10^{-5}	24.8	7.70×10^{-5}	23.3
Convection (hot)		1.10×10^{-4}	38.8	1.14×10^{-4}	35.3	1.01×10^{-4}	30.5
Fouling	Fe_3O_4	6.56×10^{-6}	2.3	6.56×10^{-6}	2.0	6.56×10^{-6}	2.0
	$(Fe,Cr)_xO_4$	3.61×10^{-6}	1.3	3.61×10^{-6}	1.1	3.61×10^{-6}	1.1
	Non-wetting	3.62×10^{-5}	12.7	7.03×10^{-5}	21.8	9.47×10^{-5}	28.6
Total		2.84×10^{-4}	100	3.22×10^{-4}	100	3.31×10^{-4}	100

Fig. 4(a). Interior of the pipe (5 cm I.D.) after the first run at low oxygen concentration.

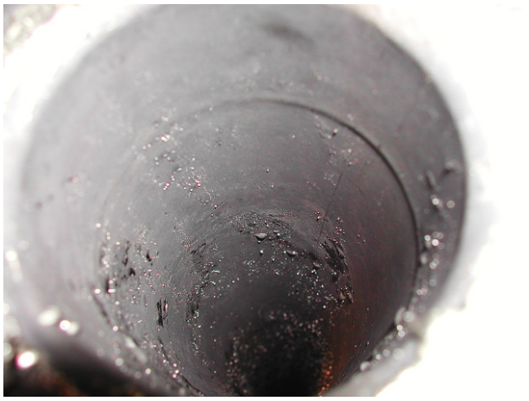

Fig. 4(b). Interior of the pipe (5 cm I.D.) after the second run at a higher oxygen concentration.

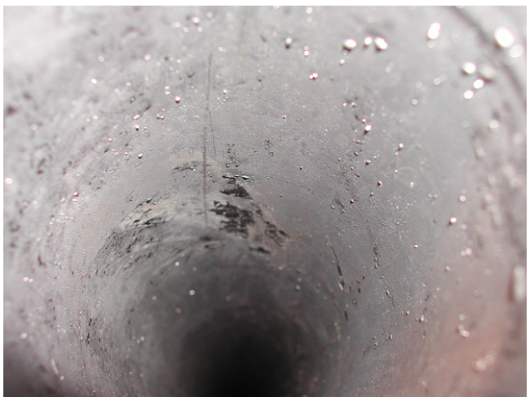

Fig. 4(c). Interior of the pipe (5 cm I.D.) after the third run at the highest oxygen concentration, showing significant oxidation and evidence of non-wetting.

maximum as the oxygen in the liquid–metal is at solubility limit. The non-wetting condition and impurities and gas trapped at non-wetting solid–liquid interfaces are the primary factors in reducing heat transfer and increasing fouling.

4. Conclusions

Results of this research reveal that the fouling factor increases with the oxygen concentration in LBE. The introduction of oxygen will enhance the generation of oxide film and therefore reduce the amount of wetting in the pipe over time. The non-wetting condition and impurities and gas trapped at non-wetting solid–liquid interfaces are the primary factors in reducing heat transfer and increasing fouling. The fouling will reach maximum as the liquid–metal is saturated with oxygen. The correlation between the fouling factor and oxygen concentration can be used to evaluate the fouling caused by oxygen in the liquid–metal. The application of LBE as a coolant in nuclear system requires a comprehensive consideration of the effects of oxygen on corrosion resistance and thermal resistance.

References

[1] N. Li, J. Nucl. Mater. 300 (2002) 73.
[2] D.Q. Kern, R.E. Seaton, Br. Chem. Eng. 4 (5) (1959) 258–262.
[3] W. Ebert, C.B. Panchal, in: Engineering Foundation Conference on Fouling Mitigation of Heat Exchangers, California, 18–23 June 1995.
[4] T. Schwarz, Exp. Thermal Fluid Sci. (25) (2001) 319.
[5] E.F.C. Somerscales, HTD 35 (1984).
[6] L.F. Melo, J. de D.R.S. Pinheiro, HTD 35 (1984).
[7] N. Li, K. Woloshun, et al., Lead–bismuth eutectic (LBE) materials test loop (MTL) Test Plan v2.0, LA-UR-01-4866, LANL, 2001.
[8] C. Ammerman, Recuperator analysis for the LBE material test loop, LA-UR-02-1863, LANL, 2000.
[9] F.P. Incropera, D.P. Dewitt, Fundamentals of Heat and Mass Transfer, John Wiley & Sons, New York, 1996.
[10] R.A. Seban, T.T. Shimazaki, Trans. ASME 73 (1951) 803.
[11] S. Kakac, R.K. Shah, W. Aung, Handbook of Single-phase Convective Heat Transfer, 1987, p. 8.1, 8.9, 8.23.
[12] O.J. Foust, Sodium–NaK Engineering Handbook II, 1976, p. 105, 106, 204.
[13] T.W. Darling, N. Li, Oxygen concentration measurement in liquid Pb–Bi eutectic, LA-UR-02-3036, LANL, 2002.
[14] F. Balbaud-Celerier, A. Terlain, P. Fauvet, C. Richet, Corrosion of steels in liquid lead alloys protected by an oxide layer application to the MEGAPIE target and to the russian reactor Concept BREST 300, Report Technique RT-SCCME 630, CEA Report 2003.
[15] J. MΦlgaard, W.W. Smeltzer, J. Appl. Phys. 42 (9) (1971) 3644.
[16] W.L. Headrick, R.E. Moore, M. Karakus, X. Liang, Characterization and structural modeling of magnesia–alumina spinel glass tank refractories, Final Report October 1, 2001–October 1, 2003, supported by the US DOE Award No. DE-FC07-01ID14250.